IET Communications

Research Article

IET Journals
The Institution of Engineering and Technology

Multiple-input multiple-output symbol rate signal digital predistorter for non-linear multi-carrier satellite channels

ISSN 1751-8628
Received on 20th February 2015
Revised on 9th July 2015
Accepted on 10th August 2015
doi: 10.1049/iet-com.2015.0176
www.ietdl.org

Efrain Zenteno[1,2] ✉, Roberto Piazza[3], M.R. Bhavani Shankar[3], Daniel Rönnow[1], Björn Ottersten[3]

[1]*Department of Electronics, Mathematics and Natural Sciences, University of Gävle, Sweden*
[2]*Department of Signal Processing, The Royal Institute of Technology KTH, Stockholm, Sweden*
[3]*Interdisciplinary Centre for Security, Reliability and Trust (SnT), University of Luxembourg, Luxembourg*
✉ *E-mail: efnzeo@hig.se*

Abstract: A digital predistortion (DPD) scheme is presented for non-linear distortion mitigation in multi-carrier satellite communication channels. The proposed DPD has a multiple-input multiple-output architecture similar to data DPD schemes. However, it enhances the mitigation performance of data DPDs using a multi-rate processing algorithm to achieve spectrum broadening of non-linear operators. Compared to single carrier (single-input single-output) signal (waveform) DPD schemes, the proposed DPD has lower digital processing rate reducing the required hardware cost of the predistorter. The proposed DPD outperforms, in total degradation, both data and signal DPD schemes. Further, it performs closest to a channel bound described by an ideally mitigated channel with limited maximum output power.

1 Introduction

The increasing need for power/mass efficient satellite transponders is pushing the use of joint amplification of multiple-carrier signals with a single high-power amplifier (HPA). In this multi-carrier (MC) scenario, several signals are multiplexed in frequency and share the on-board hardware of the satellite transponder [1]. However, the amplified signals will be distorted by the non-linear HPA. In addition to the non-linear distortions present in single carrier, the MC scenario presents adjacent channel interference (ACI) and intermodulation distortion (IMD) effects [1] which further distort the signals and decrease system capacity. Hence, the mitigation of these distortions is of primary importance for the efficient operation of MC satellite systems.

The non-linear distortion mitigation techniques operating at the gateway are referred to as digital predistortion (DPD) and they have different deployment architectures. Firstly, data DPD schemes [2, 3] are multiple-input multiple-output (MIMO) (producing one predistorted stream per carrier) and operate at the symbol rate, hence requiring relatively low digital bandwidth. Secondly, signal DPD schemes [4] are single-input single-output (SISO) and operate at higher rate, thereby requiring larger digital bandwidth than data DPD. Signal DPD fully exploits the available analogue uplink bandwidth, while data DPD has access only to the channel bandwidth set by the carrier symbol rate.

This paper presents a novel model-based MIMO DPD technique for non-linear mitigation in an MC satellite channel, referred to as symbol rate signal DPD (SRS DPD). SRS DPD produces the predistorted symbols prior to the pulse-shaping filters, similarly to data DPD schemes, but it compensates for those distortion effects (out-of-band) that cannot be handled by data DPD due to the limited digital processing bandwidth. SRS DPD uses a multi-rate processing algorithm to compute basis functions that enhances non-linear mitigation features of data DPD, while it reduces the digital processing or computational complexity compared to signal DPD. Therefore, SRS DPD provides a 'fusion' architecture to exploit bandwidths larger than data DPD at a complexity lower than signal DPD. In particular, SRS DPD compensates ACI and IMD using the link frequency planning. Using the frequency link planning of the carriers, the SRS predistorion scheme is potentially useful in highly efficient spectrum configurations, where the carriers are tightly spaced in frequency.

In the study [3], the authors have proposed MC predistorion of the satellite system using a multi-stage Volterra process applied at the symbol level. Cascading several Volterra filters enhances the mitigation abilities of the data-level computations, albeit at a higher computational complexity. In contrast to [3], SRS DPD uses a single Volterra filter and enhances the mitigation of the data level by a multi-rate scheme. Moreover, SRS DPD does not perform channel estimation as [3] which incurs in further complexity costs.

SRS-DPD scheme operates at the symbol level by including the pulse-shaping filters into the channel to be mitigated. This makes of SRS DPD optimal at the symbol level for receiver distortion minimisation. As the bit-error-rate (BER) performance is obtained decoding the received symbols, the operating domain of SRS DPD increases the overall link performance compared to SISO signal DPD, in which unmitigated distortions propagate through the pulse-shaping filters. Furthermore, for a given level of complexity, the SRS DPD achieves better performance than SISO signal DPD, and the computational complexity of SRS DPD does not increase with the uplink bandwidth motivating its inclusion in communication systems with large uplink bandwidth.

2 System model

The architecture of the satellite system is abstracted in Fig. 1. It involves a broadcast transmission from a single gateway to many receivers through a transparent satellite transponder. It has been argued that the system architecture in Fig. 1 can be used to enhance efficiency of several transmissions in satellite links [1].

The gateway transmits K carriers to the satellite. All the carriers are assumed to have the same rate and bandwidth and are compliant with DVB-S2 [5]. The carrier symbols $\{u_i\}_{i=1}^{K}$ have a symbol period (symbol interval) T_r. The ith carrier is independently upconverted to a frequency f_i after appropriate pulse-shaping using $w_i(t)$. The carriers are multiplexed in frequency towards occupying the uplink transmission bandwidth. For simplicity, the carriers will be equally frequency spaced by Δf Hz, such as $f_i = f_1 + (i-1)\Delta f$. At the satellite transponder, the carriers are channelised through an input multiplexing (IMUX) filter and further amplified by a non-linear HPA producing significant non-linear distortions. An output multiplexing (OMUX)

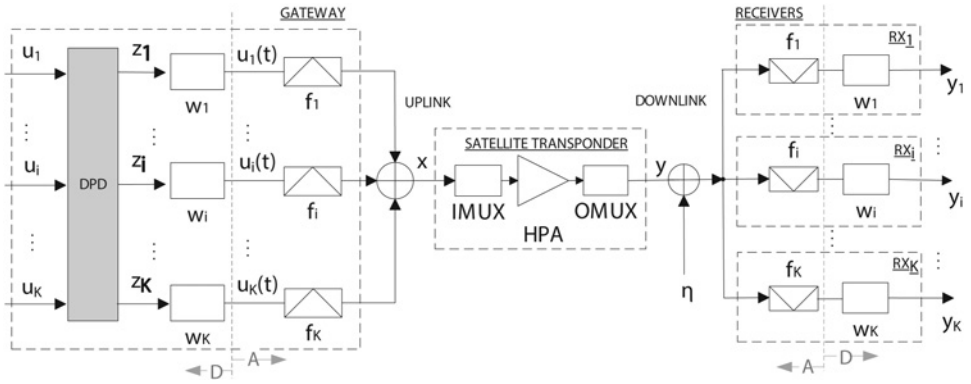

Fig. 1 *Architecture of a MC satellite system with a deployed MC predistorter. Digital (D) and Analogue (A) domains are distinguished*

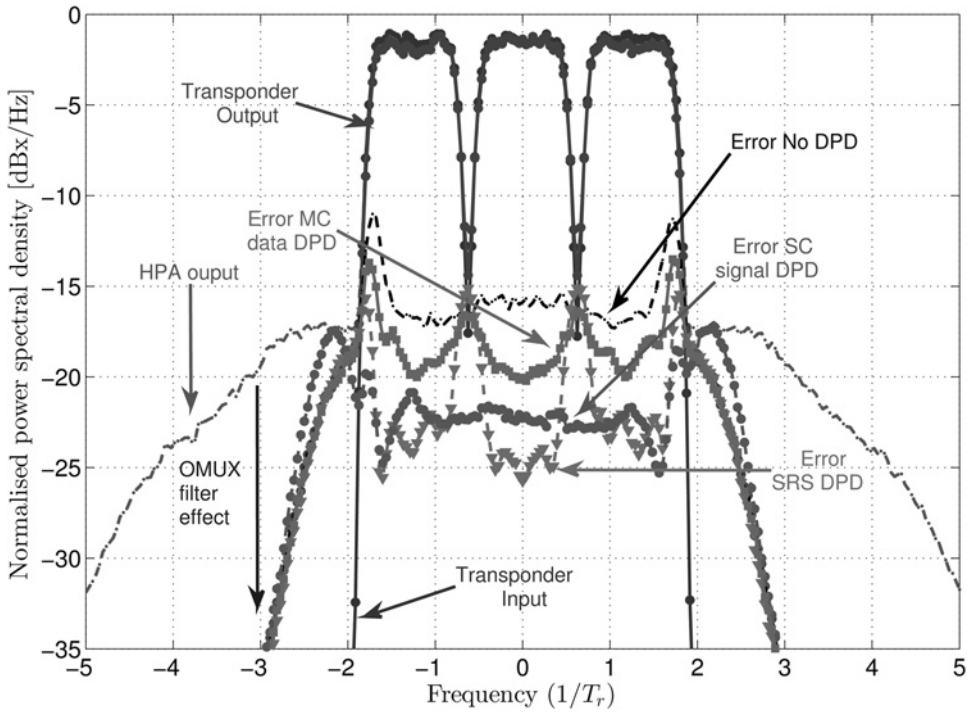

Fig. 2 *Normalised PSD of three carrier signals propagating through the satellite transponder and the error due to hardware impairments when several DPD schemes are deployed at the gateway*

filter is used to suppress the undesired spectral regrowth (out-of-band) caused by the non-linear amplification. Subsequently, the signal is corrupted with additive Gaussian noise and finally down-converted appropriately and pulse shaped independently in each receiver.

This paper considers the post-inverse of a non-linear system being equal to its pre-inverse [6]. The paper also exploits signals $u_i(t)$ (cf. Fig. 1) sampled at different rates lending a multi-rate nature to the system.

Fig. 2 shows the normalised power spectral density (PSD) of three carrier signals channelised through the satellite transponder. The carrier signals are frequency multiplexed to fill in the available bandwidth of both IMUX and OMUX filters where time and phase delay are ideally compensated. Fig. 2 depicts the changes of the PSD as the signals propagate through the satellite transponder. Fig. 2 also shows the error caused by the satellite transponder impairments when different DPD schemes are deployed at the gateway, which will be described below. Note that the HPA produces significant out-of-band emissions which are reduced by the OMUX filter. However, without DPD, the in-band distortions are still significant as observed in Fig. 2. These in-band distortions cause degradation of the communication quality and hinder the use of higher capacity modulation schemes.

Table 1 Basis functions for the low complexity MIMO data DPD [9]

Carrier 1	Carrier 2	Carrier 3
$u_1(n)$	$u_2(n)$	$u_3(n)$
$u_1(n-1)$	$u_2(n-1)$	$u_3(n-1)$
$u_1(n-2)$	–	$u_3(n-2)$
$u_2(n)u_2(n)u_3^*(n)$	$u_1(n)u_2(n)u_1^*(n)$	$u_1(n)u_3(n)u_1^*(n)$
$u_1(n)u_3(n)u_3^*(n)$	$u_1(n)u_3(n)u_2^*(n)$	$u_2(n)u_2(n)u_1^*(n)$
$u_1(n)u_2(n)u_2^*(n)$	$u_2(n)u_3(n)u_3^*(n)$	$u_2(n)u_3(n)u_2^*(n)$

3 Conventional DPD schemes

3.1 MC data DPD

Typically satellite applications apply the mitigation scheme at the symbol level [7]. In the MC scenario described in Fig. 1, data DPD has a MIMO architecture providing a mitigated stream of symbols per carrier. Data DPD operates at the symbol rate, prior to

IET Commun., 2015, Vol. 9, Iss. 16, pp. 2053–2059

the pulse-shaping filters; thereby, requiring low computational resources. However, the scheme offers limited mitigation features due to lack of bandwidth expansion needed to represent non-linear operations. MC data DPD is dual of the equalisation in [1] and can be defined using similar expressions. Several data DPD schemes for MC satellite channels are reported in the literature. E. g., data DPD based on direct learning [8], and low complexity schemes [9]. The latter form the mitigated symbols using a linear combination of the basis indicated in Table 1.

3.2 Single-carrier (SC) signal DPD

The SC signal DPD operates at higher rate, referred to as waveform domain. In the MC scenario, SC signal DPD operates with a digital processing rate $1/T_s$ in which all carrier signals are digitally combined before up-conversion. This implies different hardware architecture compared to data DPD schemes. The digital processing rate $1/T_s$ is much higher than the symbol rate $1/T_r$; first, to allocate K frequency adjacent carriers and secondly to include pth order non-linear effects ($1/T_s \simeq pK/T_r$). Hence, computational requirements are high. Note that, signal DPD in the MC scenario is band limited [10] to comply with the tight specifications of uplink bandwidth in the satellite system [5]. SC signal DPD schemes are based on SISO Volterra series [6] and pruned versions of it, which are extensively studied [11, 12]. SC signal DPD for MC satellite channels was proposed in [4] and extended in [13, 14].

In this paper, we will use a generalised memory polynomial (GMP) model [11] for the SC signal DPD. The GMP model is preferred since it has been pointed as a model structure which performs with lower error model for the same level of computational complexity when compared to other model structures [15]. Furthermore, the GMP can model the inverse of the satellite transponder structure to be mitigated [16]. That is, a non-linear static block sandwiched between two linear dynamic filters [11].

The GMP is described by the input–output relationship [11]

$$y(nT_s) = \sum_{p=1}^{[(P+1)/2]} \sum_{m_1,m_2}^{M_1,M_2} h_{2p-1}^{(m_1,m_2)} x(nT_s - m_1)\left|x(nT_s - m_1 - m_2)\right|^{2(p-1)}, \tag{1}$$

where $\sum_{m_1,m_2}^{M_1,M_2}$ denotes the double sum over the integers m_1 and m_2, respectively. M_1 and M_2 denote the memory depths, $h_{2p-1}^{(m_1,m_2)}$ are the model parameters, and P is an odd integer denoting the non-linear model order. The signals $x(nT_s)$ and $y(nT_s)$ are frequency multiplexed input and output of the satellite transponder (cf. Fig. 1).

4 MIMO SRS DPD

Model-based DPD mitigation techniques for non-linear MIMO systems are constructed using the MIMO Volterra [17] series. The series builds on polynomial expansions of the inputs $\{u_i(t)\}_{i=1}^K$, i.e. terms like $u_1(t)u_3(t)u_2^*(t)$ [18, 19], where * denotes the complex conjugate. Such product terms yield a signal at the DPD output whose bandwidth stretches beyond that of $u_i(t)$. In fact, the bandwidth expansion due to a polynomial operation depends on its order [16]. Since the processing bandwidth in MIMO data DPD schemes is limited by the carrier symbol rate, and hence the bandwidth per carrier, MIMO data DPD is unable to capture these distortion effects.

Using a novel multi-rate algorithm for predistorter computation, SRS-DPD captures aforementioned distortion effects, which lie outside of the band considered in data DPD schemes. The technique is detailed next: Fig. 3 exemplifies the SRS-DPD scheme in the frequency domain using a three-carrier system and a third-order non-linear compensation. In this paper, SRS-DPD computes third order MIMO non-linear terms of Volterra series

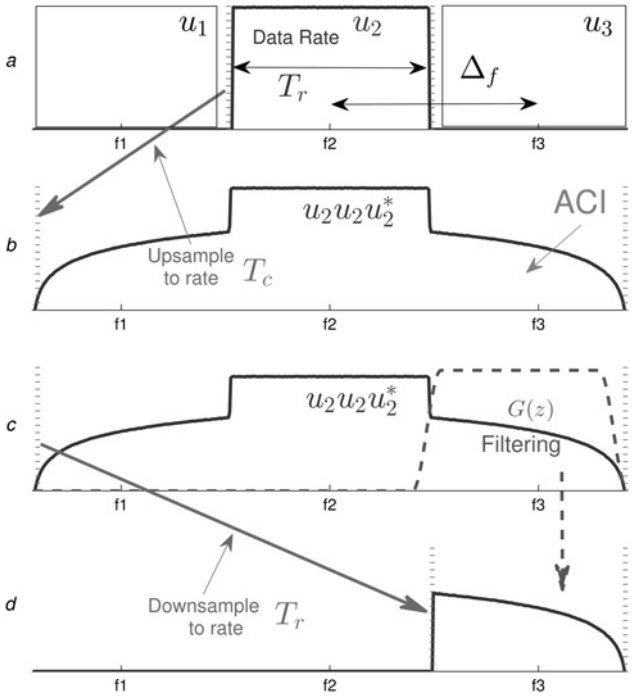

Fig. 3 *Illustration of the SRS-DPD algorithm in frequency domain. The SRS DPD base {2, 2, 2} (cf. Table 2) at the i = 3 carrier*

a Carriers at data rate
b Up-sampled carriers and operated by $u_2u_2u_2^*$
c Frequency shifted and filtered to keep the contribution to carrier $i = 3$
d Down-sampled signal at data rate. Vertical dashed lines indicate the digital processing bandwidth

(cf. Table 2). Further, using the carrier frequency plan, it isolates the distortion terms from the MIMO Volterra series to each carrier, as indicated in Fig. 3*c*. The distortion effects modelled by the MIMO Volterra series can be classified as IMD, ACI, ISI and self-interference. The example in Fig. 3 depicts ACI from the inner carrier that is added in the predistorter of the outer carrier at data rate $1/T_r$ (cf. Fig. 3*d*).

SRS DPD enhances the mitigation performance of data DPD similarly to signal DPD schemes. However, SRS DPD requires lower digital processing rate than signal DPD. The SRS-DPD processing rate is $1/T_c = q/T_r$ where q is set to enlarge the processing bandwidth to compute non-linear products affecting adjacent carriers. q must be set according to the frequency carrier spacing Δf and the non-linear order p considered in the compensation. In particular, $q = \left\lceil p\dfrac{\Delta f}{T_r} \right\rceil$, with $\lceil\cdot\rceil$ denoting the maximum integer operator. For spectrally efficient like MC signals, $q \simeq p$. Hence, SRS-DPD digital processing rate is $1/T_c \simeq p/T_r$. On the other hand, the signal DPD processing rate is given by

Table 2 Indexes $\{i_1, i_2, i_3\}$ of the third non-linear order contributors $u_{i_1}u_{i_2}u_{i_3}^*$ in three-carrier system at ith carrier

$f_{i_1} + f_{i_2} - f_{i_3} - f_i$	$i = 1$	$i = 2$	$i = 3$
$-\Delta f$	–	{1, 1, 1}	{1, 2, 1}
	{1, 1, 2}	{1, 2, 2}	{1, 3, 2}
	{1, 2, 3}	{1, 3, 3}	{2, 2, 2}
	–	{2, 2, 3}	{2, 3, 3}
0	{1, 1, 1}	{1, 2, 1}	{3, 3, 3}
	{1, 2, 2}	{1, 3, 2}	{3, 2, 2}
	{1, 3, 3}	{2, 2, 2}	{3, 1, 1}
	{2, 2, 3}	{2, 3, 3}	{2, 2, 1}
Δf	{1, 2, 1}	{3, 3, 3}	–
	{1, 3, 2}	{3, 2, 2}	{3, 3, 2}
	{2, 2, 2}	{3, 1, 1}	{3, 2, 1}
	{2, 3, 3}	{2, 2, 1}	–

$1/T_s \simeq pK/T_r$, where K is the number of carriers. Hence, $1/T_s \geq 1/T_c$ which points out the lower digital rate required in SRS DPD compared to signal DPD. Thus, SRS DPD combines salient features of data and signal DPD. It processes wider bandwidth like signal DPD while retaining MIMO architecture of data DPD (i.e. it produces predistorted symbols streams per carrier that mitigate the non-linear distortion in the channel).

SRS DPD involves linear and third-order functions of data on different carriers. The construction of the SRS basis functions (columns in the linear regression matrix) can be summarised by:

Linear contribution

Form the linear basis as $u_i(nT_r - m_1)$ using memory depth $m_1 = 0, \ldots, M_1$, for all carriers.

Third-order contribution

The basis functions for the ith carrier are formed as:

- Up-sample the carriers to a rate $1/T_c = q/T_r$, with $q \in \mathbb{N}$ forming $u_i(nT_c)$.
- Form the terms $u_{i_1}(nT_c - m_1)u_{i_2}(nT_c - m_2)u^*_{i_3}(nT_c - m_3)$ as depicted in Fig. 3*b*) for $\{i_1, i_2, i_3\}$ in Table 2 using memory depths $m_k = 0, \ldots, M_3$.
- Frequency shift (by $f_{i_1} + f_{i_2} - f_{i_3} - f_i$) the terms, such that they are centred to frequency f_i. For equally spaced carriers, the frequency shift can be $\{0, \pm\Delta f, \pm 2\Delta f, \ldots\}$. IMD has a 0 shift, while ACI have a shift of $\pm\Delta f$ [1].
- Filter with $g_i(nT_c)$ to retain only the in-band contribution to the ith carrier (cf. Fig. 3*c*).
- Form a new basis by down-sampling the filtered sequences to symbol rate T_r (cf. Fig. 3*d*).

This process can be formalised by,

$$\begin{aligned} z_i(nT_r) = & \sum_{i_1=1}^{K} \sum_{m_1=0}^{M_1} h^{(1)}_{i_1,i}(m_1) u_{i_1}(nT_r - m_1) \\ & + \sum_{i_1,i_2,i_3=1}^{K} \sum_{m_1,m_2,m_3=0}^{M_3} h^{(3)}_{i_1,i_2,i_3,i}(m_1, m_2, m_3) \\ & \times \boldsymbol{D}\{u_{i_1}(nT_c - m_1)u_{i_2}(nT_c - m_2)u^*_{i_3}(nT_c - m_3) \\ & \times e^{j2\pi(f_{i_1}+f_{i_2}-f_{i_3}-f_i)nT_c} \otimes g_i(nT_c)\} \end{aligned} \quad (2)$$

where $z_i(nT_r)$ is the nth predistorted symbol for the ith carrier, $h^{(1)}_{i_1,i}(m_1)$ and $h^{(3)}_{i_1,i_2,i_3,i}(m_1, m_2, m_3)$ are the linear and third-order kernels, respectively, $\boldsymbol{D}\{\cdot\}$ denotes the down-sampling operator from a rate of T_c to T_r and $\otimes$ is the convolution operator. The filter $g_i(nT_c)$ isolates the distortions contributing to the ith carrier (cf. $G(z)$ in Fig. 3*c*); rendering an alias-free down-sampling operation. A natural choice for $g_i(nT_c)$ is the pulse-shaping filter $w_i(nT_c)$.

To enhance mitigation properties in SRS DPD, the up-sampling process can be made by zero-padding the data symbols and pulse-shaping with $w_i(nT_c)$. Clearly these mechanisms will not alter the bandwidth of the underlying signal [20]. The use of the filter $w_i(nT_c)$, in the up-sampling and in the distortion isolation in Fig. 3*c*) is equivalent to perform DPD at the data level (including both transmitter and receiver pulse-shaping filters into the channel) but taking into account the PSD spread caused by the non-linear operators. Hence, the distortion produced by the *coupling* of the non-linearity with the pulse shape filters is then accounted in the DPD. This enhances the distortion mitigation features of the proposed technique. In the evaluation, we use only the steady-state response from the filter $w_i(nT_c)$.

The down-sampling process described in the SRS DPD technique (3d) is described only for pedagogical reasons. From Fig. 1, the output of the predistorter is to be pulse-shaped and thus requires to be upsampled. Hence, the down-sampling is not required and can be removed in the implementation by integrating the SRS predistorter block with the pulse-shaping filters. This is possible since these stages are deployed in digital domain depicted in Fig. 1.

Table 3 Simulation settings of a three-carrier satellite channel

signal	modulation format	32 APSK
	symbol rate ($1/T_r$)	7 M symbols/s
	carrier spacing	$1.25/T_r$
	coding scheme	LDPC 9/10
	LDPC iterations	50
channel	pulse-shaping filter	SRRC ρ = 0.25
	IMUX – OMUX 3 dB band	26–32 MHz
	simulation rate	$20/T_r$
	HPA	Saleh's model

Not all third-order MIMO Volterra basis need to be considered in the mitigation technique. Some of these basis in (2) lie outside of the band of interest, i.e. outside the pass-band of the OMUX filter, these can be discarded without loss in performance. For instance, the base $\{1, 1, 3\}$ contributes to the frequency $f_1 + f_1 - f_3 = f_1 - 2\Delta f$, that is outside of the considered band of the system. Table 2 shows the in-band contributing basis of the three equally frequency-spaced carriers. Table 2 is symmetric with respect to $\pm\Delta f$ as third order non-linear basis contribute equally to both adjacent carriers. The terms in Table 2 are in agreement with those presented in [1].

Note that the predistortion process in (2) is linear in the parameters (the Volterra kernels). Hence, its estimation can be made using linear regression techniques which are mature and robust implementations are readily available. In this work, we have use the indirect learning architecture as described in [11] to estimate the Volterra kernels required in the SRS predistorter.

5 Performance analysis

A satellite system of $K = 3$ carrier signals was considered with a transponder simulated as the cascade of an IMUX filter, a HPA and an OMUX filter. The IMUX and OMUX filters were modelled by FIR structures using 51 and 41 taps at the simulation frequency, respectively. The HPA was modelled by the static non-linear Saleh model, described by amplitude distortion $A(z) = \alpha_0 z/(1 + \alpha_1 z^2)$, and phase distortion $\Gamma(z) = \beta_0 z^2/(1 + \beta_1 z^2)$ [21], where z is the amplitude of the base-band signal at the input of the HPA, that is, $z = |x|$ (cf. Fig. 1), with $\alpha_0 = 2$, $\alpha_1 = 1$, $\beta_0 = \pi/6$, and $\beta_1 = 1$. Table 3 summarises the settings of the simulations. The LDPC code in Table 3 is representative of the state-of-the-art in satellite systems [22].

All studied predistorters were identified using linear least-square estimation by interchanging the input and output in their respective models, as suggested by the indirect learning architecture [23]. The identification used a low-noise received signal; this assumes the existence of an MC receiver deployed as a reference terminal, providing data for identification [9].

The error vector magnitude (EVM) in dB is used to evaluate the uncoded satellite link, $\text{EVM} = -10\log_{10}(P_{\text{error}}/P_s)$, where P_{error} is the average energy of the error signal, defined as the difference between the received symbol to the corresponding constellation value. P_s is the average energy in the constellation. The total degradation (TD) is used to evaluate the performance in the coded satellite links. TD accounts for the non-linear distortion and penalises the loss in HPA power efficiency by including the output power back-off (OBO) [24],

$$\text{TD}_i = \left[\frac{E_s}{N_0}\right]_i^{\text{NL}} - \left[\frac{E_s}{N_0}\right]_i^{\text{L}} + \text{OBO} \quad (3)$$

OBO is defined as the ratio of the output power of an SC at saturation to the total power of the output signal in the specified conditions, $[E_s/N_0]_i^{\text{NL}}$ and $[E_s/N_0]_i^{\text{L}}$ are the average symbol energy to noise ratios required to achieve a target BER in the non-linear channel and the linear channel (AWGN), respectively, for the ith carrier. While E_s/N_0 is an SC metric, the OBO depends on the combined signal and not on individual carriers (aggregate OBO). In the simulations, a target BER of 10^{-5} was used.

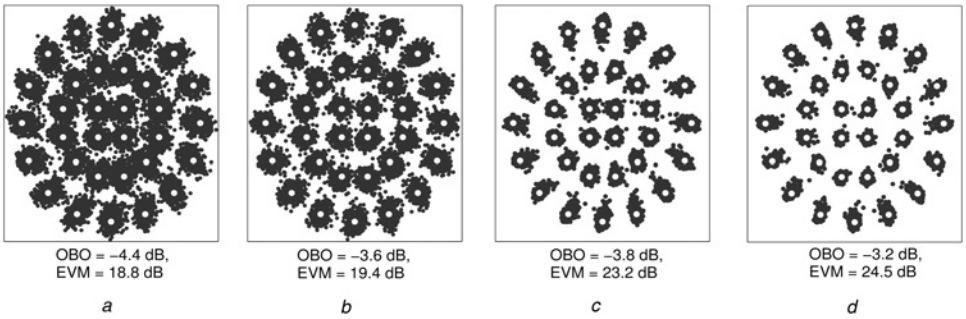

Fig. 4 *Noiseless received symbols of the inner carrier*

a No compensation
b MIMO data DPD [9]
c SISO signal DPD [4]
d Proposed MIMO SRS DPD

We compare three DPD schemes: MIMO data DPD [9], SC signal DPD [4] and the proposed SRS DPD. All these DPD schemes use a non-linear order $p = 3$. The MIMO data DPD [9] uses linear dynamic and third-order static compensation terms in its model, according to Table 1. SC signal DPD uses the model described by (1) with $M_1 = 6$, $M_2 = 2$. Finally, SRS DPD uses the model described by (2) with $M_1 = 3$ and $M_3 = 1$. To use the same time spam during DPD identification, all MIMO data DPD schemes use 3800 symbols per carrier whereas the SISO signal DPD uses 49,400 samples of the single waveform stream. Note that, the low number of symbols in the identification of the SRS DPD reduces its computational complexity requirements and it is competitive with state-of-the-art predistortion schemes [3, 14].

To focus on non-linear distortions, in the simulations all the unmitigated (No DPD) streams are always compensated using 1 tap equaliser. Fig. 4 shows the noiseless received symbols of the outer carrier without compensation and with the different DPD schemes studied. For each scheme, the HPA in the satellite transponder is operated at optimal OBO. That is, the operation OBO that minimises the TD of the satellite link. Fig. 4 reports the obtained EVM at optimal OBO. It is clear that both SC signal DPD and the proposed SRS DPD achieves enhanced levels of mitigation.

As SC signal DPD operates at a higher rate, it requires larger memory depth compared to data DPD schemes. The memory depth is required to compensate the frequency variations encountered in the channel produced by the sharp transition bands of the IMUX and OMUX filters as seen in the error PSD in Fig. 2. The increased memory depth in the SC signal DPD model complicates the identification and has a negative impact on the complexity and performance, particularly for the outer carriers. Aiming to alleviate this problem, linear filtering combined with non-linear operations has been proposed to enhance the performance of SC signal DPD [13, 14]. This requires two measurements of different output power in the HPA to identify the combined linear response of the filters. As linear filtering is embedded into the proposed SRS DPD, it combats, to large extent, the linear degradations of the channel. Furthermore, SRS DPD performs a single step of processing and does not require to changing the operating conditions of the satellite transponder as in [13].

The error PSD of the investigated DPD schemes is shown in Fig. 2. All the three DPD schemes reduce the in-band error compared to the case of no DPD. The MC data DPD and SRS DPD have error PSD with peaks between the bands (inter-band error), whereas the SISO signal DPD gives a more even error PSD. The difference in the error PSD reflects the fact that the former are MIMO methods mitigating solely the in-band and the latter is a SISO method mitigating the whole uplink bandwidth. The SRS-DPD achieves, however, lower in-band error than the SC signal DPD.

Fig. 5 shows the coded BER results versus average symbol energy to noise ratios (E_s/N_0) for the studied DPD schemes when the HPA is operated at 3.8 dB of OBO. The losses observed without compensation scheme are large and justify the deployment of mitigation techniques. Further, MC data DPD has a limited compensation ability while SC signal DPD and SRS DPD have enhanced performance as depicted in Fig. 5.

Table 4 shows the different features and performance results for each scheme. Note the different digital processing rate of each scheme, the MIMO data DPD scheme operates at a rate of $1/T_r = 7$ M samples/s, SRS DPD does at a rate of $4/T_r = 28$ M samples/s, while SC signal DPD does at the highest rate of $13/T_r = 91$ M samples/s.

The MIMO architecture of SRS DPD makes the number of basis functions larger as compared to SC signal DPD. This is because the basis in MIMO Volterra series are all permutations of the inputs in the MIMO channel; which became a single input for the SC signal DPD. However, the basis functions for the MIMO SRS predistorter are redundant. E.g., from the 32 basis reported in Table 2 only 16 are unique and need to be computed. The total number of basis of the three-carrier MIMO series correspond to 210 with 126 unique basis indicated by Table 4. This redundancy is due to the frequency symmetry of the output of non-linear operators which can be exploited to reduce the SRS predistorter computation, similarly to the reductions pointed in [3].

Due to the different deployment architectures (SISO and MIMO), model structure and digital processing rate, the comparison of the studied DPD schemes is not straightforward. In particular, the

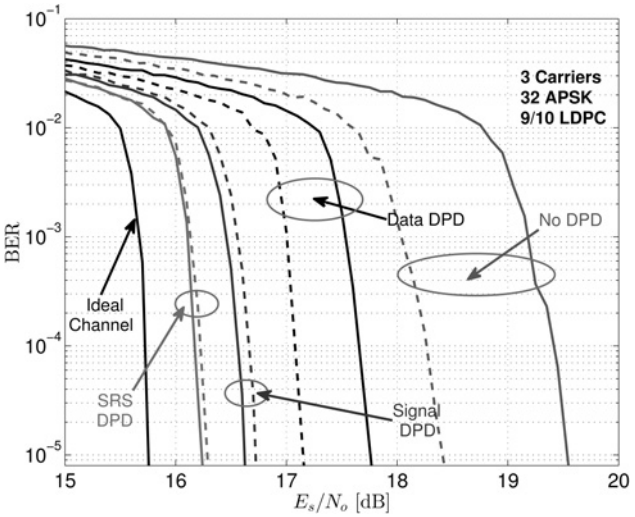

Fig. 5 *BER against E_s/N_o for different DPD mitigation schemes studied, inner carrier in dashed lines, outer carrier in solid lines. The HPA is operated at 3.8 dB of OBO*

Table 4 Comparison of third order non-linear mitigation schemes in a three-carrier uncoded satellite link using 32 APSK 9/10 LDPC per carrier and HPA operated at OBO of 3.8 dB

DPD scheme	Settings	DSP rate	No. of basis functions	rel. FLOPS	EVM outer, dB	EVM inner, dB
no mitigation	–	–	–	–	17.6	18.2
MIMO data [9]	Table 1	$1/T_r$	17	1	19.9	20.9
MIMO SRS	equation (2) $M_1 = 3$, $M_3 = 1$	$4/T_r$	126	26	26.8	26.3
SISO signal [4]	equation (1) $M_1 = 6$, $M_2 = 2$	$13/T_r$	62	55	24.0	24.2

predistorter computation is tied to the DPD scheme used. E.g., the low-complexity MIMO data DPD [9] has a total of 17 basis functions, while SRS DPD and signal DPD have a total of 126 and 62 basis functions, respectively. Thus, the floating point operations per second (FLOPS) combine the digital processing rate of a DPD scheme with its specific predistorter computation (number of operations). Thus, the FLOPS provides a unique metric to evaluate the computational complexity of DPD schemes that operate with different sampling rates, model structures and system architectures.

The performance is evaluated using the EVM of the noiseless received symbols at an OBO of 3.8 dB and the ratio of number of FLOPS relative to MC data DPD which presents approximately a total of 1700 M FLOPS [9]. Data DPD achieves an EVM enhancement of around 2.5 dB compared to a non-mitigated stream, while SRS DPD and signal DPD achieve around 8 and 6 dB of improvement, respectively. The number of FLOPS increases by 26 times from MC data DPD to SRS DPD with an EVM enhancement of around 6 dB. However, an increase of more than two times of FLOPS from SRS DPD to SC signal DPD does not result in any EVM performance enhancement. Signal DPD shows increased complexity, seen in the FLOPS, that is mostly due to its higher processing rate compared to other DPD schemes. The EVM level reported in Table 4 can also be appreciated in Fig. 2. As observed in the error PSD in Fig. 2, MC data DPD and SRS DPD mitigate solely the in-band distortions while SC signal DPD mitigates both in-band and inter-band distortions, the latter are irrelevant at the receivers. The computational complexity (FLOPS) in Table 4 compares a pruned SISO Volterra model (low complexity GMP) for SC signal DPD with the MIMO Volterra series in the proposed SRS DPD. In this case, the computational complexity favours the MIMO Volterra because of the large memory requirements in the SC signal DPD. Furthermore, pruned model structures can be used for the SRS-DPD scheme. These pruned forms of MIMO series will further reduce the computational complexity requirements of the proposed SRS-DPD scheme.

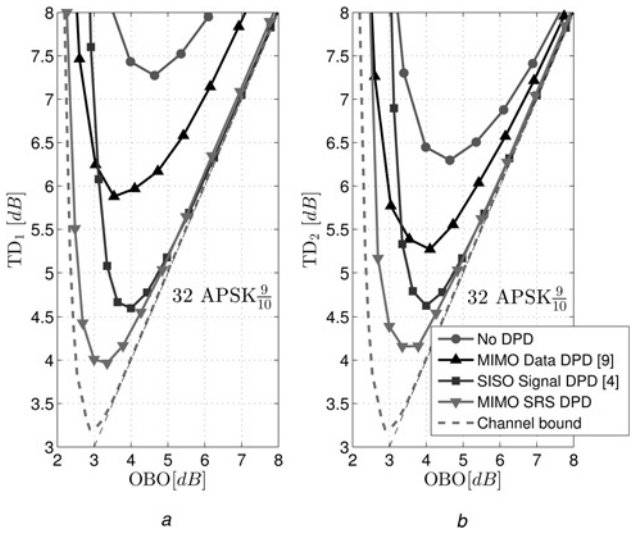

Fig. 6 *TD performance comparison for different DPD schemes. The satellite link uses a three-carrier 32 APSK LDPC-9/10 (Table 3)*

a Outer carrier
b Inner carrier

The enhanced EVM performance of SRS DPD is due to the fact that SRS DPD minimises the receiver distortion at symbol level. Hence, it is optimal for the EVM of the received symbols. In contrast, SC signal DPD is optimal at the waveform level, and thus, the uncompensated error in the DPD propagates through the pulse-shaping filters and appears as distortion in the received symbols. Moreover, in the described satellite scenario, the overall BER link performance is evaluated after decoding the received symbols, which where optimally mitigated in the SRS-DPD scheme. In consequence, the SRS DPD enhances the coded link performance compared to signal DPD.

Note that the high digital processing rate of SC signal DPD is required to represent the non-linear effects of the frequency multiplexed (enlarged) signal. In general, a K MC signal with carriers equally spaced by Δf, with symbol rate $1/T_r$ and pulse-shaped with a filter roll-off ρ for all carriers has the analogue bandwidth of $[(K-1)\Delta f + 1/T_r](\rho+1)$ Hz. This bandwidth is further increased by a factor p denoting the non-linear order considered in the SC signal DPD predistorter. Using the simulation settings indicated by Table 3 yields a processing rate of 13 times larger than the data rate for SC signal DPD using a third-order non-linear compensation scheme.

Fig. 6 shows the coded TD versus the aggregated OBO. Unmitigated (No DPD) carriers have large degradation and different levels of TD, depending on the carrier location, i.e. inner or outer. MC data DPD enhances the TD performance, but, it still has a performance that is carrier dependent, which indicates unmitigated distortions. From Fig. 6, both SC signal DPD and SRS DPD have an enhanced level of TD that is independent of the carrier location. However, signal DPD has larger OBO losses when compared to the proposed SRS DPD, which reduces its optimal TD operating OBO (cf. Fig. 6). This behaviour of signal DPD is caused by the amplitude expansion in the predistorted signal worsening the channel distortions. It is expected that this detrimental effect can be alleviated by the use of peak reduction techniques [25]. However, the optimal setting of peak reduction techniques for signal DPD is not straightforward and some compromises have to be considered [26]. On the other hand, the OBO losses in the proposed SRS-DPD scheme are smaller to those encountered in signal DPD, enhancing the TD performance in low operating OBOs.

Fig. 6 also depicts a TD bound (channel bound) given by a perfectly linear channel with limited output power. Such a channel is linear up to a saturation point where an ideal clipping function occurs. This behaviour is expected in perfectly linearised realistic satellite transponders [24] and serves as a bound for an ideal DPD. Clearly, among the studied predistorters, SRS DPD is the one closest to the ideal DPD bound.

The proposed SRS-DPD scheme can be used when the carriers have different data rates. In this case, the up-sampling factor for the ith carrier denoted q_i is chosen such that all up-sampled carriers have a common sampling time scale. The up-sampled data are then processed accordingly to the SRS scheme. Note that q_i does not need to be integer and efficient signal processing can be performed using poly-phase interpolators. For a spectral-efficient MC scenario, where carriers are closely spaced in frequency, the basis functions of the SRS DPD can be augmented with the signals leaking from adjacent carriers into the ith pulse-shape

IET Commun., 2015, Vol. 9, Iss. 16, pp. 2053–2059

Table 5 Number of basis functions in a third-order SRS DPD $M_1 = 3$, $M_3 = 1$ using a full and diagonal Volterra series and its EVM performance comparison

No. of carriers	Full Volterra	Diagonal Volterra	Degradation Δ EVM, dB
2	76	36	0.1
3	210	76	0.2
4	428	184	0.2
5	866	302	0.1

filter. This is equivalent to the proposed scheme in Fig. 3 using linear operators which captures the linear leakage of the adjacent carriers for distortion mitigation.

Despite of the level of redundancy in the SRS predistorter, the computational complexity savings (measured in FLOPS) from the SRS DPD compared to SC signal DPD will reduce with an increasing number of carrier signals. This is because of the dramatic increase in the number of basis functions with an increasing number of carrier signals as shown in Table 5. This results from the MIMO Volterra series expansion considering permutations of all carriers [9]. However, the computational complexity of proposed technique can be further reduced by pruning the MIMO Volterra series, for instance, using memory polynomials that consider solely the diagonal kernels of the series [27] or using basis pursuit approaches [28]. A significant number of basis functions can be discarded with minor performance degradation using solely the diagonal terms in the MIMO Volterra series as shown in Table 5. The worst-case degradation in EVM for all the carriers (due to the model pruning) is indicated in the last column of this table.

6 Conclusions

A novel DPD technique namely SRS DPD is presented for a satellite link employing MC operations. SRS DPD combines salient features of MIMO data DPD and SC signal DPD and outperforms both of them in terms of EVM and TD. SRS DPD relies on a multi-rate approach and uses the frequency link planning to accurately describe the effects of non-linear distortions in a MC scenario. This approach enables the operation of the satellite transponder at lower OBOs while requiring lower digital processing rate compared to SC signal DPD.

The MIMO architecture of SRS DPD contrasts with the SISO architecture of signal DPD implying different hardware deployments. However, the sampling rate required in signal DPD increases with the uplink bandwidth of the system, while SRS-DPD rate does not. These motivate the use of SRS DPD in systems with large uplink bandwidths like the envisaged high throughput satellite links.

7 References

1 Beidas, B.F.: 'Intermodulation distortion in multicarrier satellite systems: analysis and turbo Volterra equalization', *IEEE Trans. Commun.*, 2011, **59**, (6), pp. 1580–1590. ISSN: 0090-6778. doi: 10.1109/TCOMM.2011.042111.100320

2 Piazza, R., Bhavani Shankar, M.R., Zenteno, E., *et al.*: 'Multicarrier digital pre-distortion/ equalization techniques for non-linear satellite channels'. Proc. 30th AIAA Int. Communication Satellite Systems Conf. (ICSSC), Ottawa, Canada, 2012

3 Beidas, B.F., Iyer Seshadri, R., Becker, N.: 'Multicarrier successive predistortion for nonlinear satellite systems', *IEEE Trans. Commun.*, 2015, **63**, (4), pp. 1373–1382. ISSN: 0090-6778. doi: 10.1109/TCOMM.2015.2401556

4 Kelly, N., Zhu, A., Brazil, T.J.: 'Digital predistortion feasibility studies for multicarrier satellite communication systems'. Proc. 31th AIAA Int. Communication Satellite Systems Conf. (ICSSC), Florence, Italy, 2013

5 Digital Video Broadcasting (DVB); Second generation framing structure, channel coding and modulation systems for Broadcasting, Interactive Services, News Gathering and other broadband satellite applications (DVB-S2) (European Telecommunications Standards Institute (ETSI), Piscataway, NJ), 2009-08

6 Schetzen, M.: 'The Volterra and wiener theories of nonlinear systems' (Wiley & Sons, New York, 1980). ISBN: 0471044555. Available at http://www.worldcat.org/isbn/0471044555

7 Casini, E., De Gaudenzi, R., Ginesi, A.: 'DVB- S2 modem algorithms design and performance over typical satellite channels', *Int. J. Satell. Commun. Netw.*, 2004, **22**, (3), pp. 281–318. doi: 10.1002/sat.791

8 Piazza, R., Bhavani Shankar, M.R., Ottersten, B.: 'Data predistortion for multicarrier satellite channels based on direct learning', *IEEE Trans. Signal Process.*, 2014, **62**, (22), pp. 5868–5880. ISSN: 1053-587X. doi: 10.1109/TSP.2014.2358958

9 Zenteno, E., Piazza, R., Bhavani Shankar, M.R., *et al.*: 'Low complexity predistortion and equalization in nonlinear multicarrier satellite communications', *EURASIP J. Adv. Signal Process.*, 2015, **2015**, p. 30. ISSN: 1687-6172. doi: 10.1186/s13634-015-0215-0

10 Yu, C., Guan, L., Zhu, E., *et al.*: 'Band-limited Volterra series-based digital predistortion for wideband RF power amplifiers', *IEEE Trans. Microw. Theory Tech.*, 2012, **60**, (12), pp. 4198–4208. ISSN: 0018-9480. doi: 10.1109/TMTT.2012.2222658

11 Morgan, D.R., Ma, Z., Kim, J., *et al.*: 'A generalized memory polynomial model for digital predistortion of RF power amplifiers', *IEEE Trans. Signal Process.*, 2006, **54**, (10), pp. 3852–3860. ISSN: 1053-587X. doi: 10.1109/TSP.2006.879264

12 Isaksson, M., Wisell, D., Rönnow, D.: 'A comparative analysis of behavioral models for RF power amplifiers', *IEEE Trans. Microw. Theory Tech.*, 2006, **54**, (1), pp. 348–359. ISSN: 0018-9480. doi: 10.1109/TMTT.2005.860500

13 Allegue-Martinez, M., Kelly, N., Zhu, A.: 'Digital linear pre-compensation technique to enhance predistortion performance in multicarrier DVB-S2 satellite communication systems', *Electron. Lett.*, 2014, **50**, (13), pp. 957–959. ISSN: 0013-5194. doi: 10.1049/el.2014.1172

14 Kelly, N., Allegue-Martnez, M., Arapoglou, P.-D., *et al.*: 'Bandwidth-constrained digital pre-compensation technique for multi-carrier satellite communications', *Int. J. Satellite Commun. Netw.*, 2015. ISSN: 1542-0981. doi: 10.1002/sat.1106. Available at http://dx.doi.org/10.1002/sat.1106

15 Tehrani, A.S., Cao, H., Afsardoost, S., *et al.*: 'A comparative analysis of the complexity/accuracy tradeoff in power amplifier behavioral models', *IEEE Trans. Microw. Theory Tech.*, 2010, **58**, (6), pp. 1510–1520. ISSN: 0018-9480. doi: 10.1109/TMTT.2010.2047920

16 Bendat, J.: 'Nonlinear systems techniques and applications' (John Wiley & Sons, Inc., New York, 1998)

17 Swain, A.K., Billings, S.A.: 'Generalized frequency response function matrix for MIMO non-linear systems', *Int. J. Control*, 2001, **74**, (8), pp. 829–844. doi: 10.1080/00207170010030144

18 Hummels, D.R., Gitchell, R.: 'Equivalent low-pass representations for bandpass Volterra systems', *IEEE Trans. Commun.*, 1980, **28**, (1), pp. 140–142. ISSN: 0090-6778. doi: 10.1109/TCOM.1980.1094572

19 Amin, S., Landin, P.N., Händel, P., *et al.*: 'Behavioral modeling and linearization of crosstalk and memory effects in RF MIMO transmitters', *IEEE Trans. Microw. Theory Tech.*, 2014, **62**, (4), pp. 810–823. ISSN: 0018-9480. doi: 10. 1109/TMTT.2014.2309932

20 Proakis, J.G.: 'Digital signal processing: principles, algorithms, and application' (Prentice–Hall, 1996, 3rd edn.)

21 Saleh, A.A.M.: 'Frequency-independent and frequency-dependent nonlinear models of TWT amplifiers', *IEEE Trans. Commun.*, 1981, **COM-29**, (11), pp. 1715–1720

22 Digital Video Broadcasting (DVB); Second generation framing structure, channel coding and modulation systems for Broadcasting, Interactive Services, News Gathering and other broadband satellite applications; Part 2: DVB-S2 Extensions (DVB-S2X) (European Telecommunications Standards Institute (ETSI), Piscataway, NJ), 2014-10AQ

23 Eun, C., Powers, E.J.: 'A new Volterra predistorter based on the indirect learning architecture', *IEEE Trans. Signal Process.*, 1997, **45**, (1), pp. 223–227. ISSN: 1053-587X. doi: 10.1109/78.552219. 22

24 Aloisio, M., Casini, E., Ginesi, A.: 'Evolution of space traveling-wave tube amplifier requirements and specifications for modern communication satellites', *IEEE Trans. Electron. Devices*, 2007, **54**, (7), pp. 1587–1596. ISSN: 0018-9383. doi: 10.1109/TED.2007.898243

25 Nader, C., Landin, P.N., Van Moer, W., *et al.*: 'Peak- power controlling technique for enhancing digital pre-distortion of RF power amplifiers', *IEEE Trans. Microw. Theory Tech.*, 2012, **60**, (11), pp. 3571–3581. ISSN: 0018-9480. doi: 10.1109/TMTT.2012.2213836

26 Han, S.H., Lee, J.H.: 'An overview of peak-to-average power ratio reduction techniques for multicarrier transmission', *IEEE Wirel. Commun.*, 2005, **12**, (2), pp. 56–65. ISSN: 1536-1284. doi: 10.1109/MWC.2005.1421929

27 Younes, M., Kwan, A., Rawat, M., *et al.*: 'Three-dimensional digital predistorter for concurrent tri-band power amplifier linearization'. Int. IEEE MTT-S Microwave Symp. Digest (IMS), 2013, pp. 1–4. doi: 10.1109/MWSYM.2013.6697635

28 Zenteno, E., Amin, S., Isaksson, M., *et al.*: 'Combating the dimensionality of nonlinear MIMO amplifier predistortion by basis pursuit'. 44th European Microwave Conf. (EuMC), 2014, pp. 833–836. doi: 10.1109/EuMC.2014.6986564